

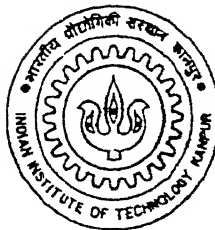
A PARTICLE DYNAMICS MODEL FOR THE EVALUATION OF THE PERFORMANCE OF A PELTON WHEEL BUCKET

*A Thesis Submitted
in Partial Fulfilment of the Requirements
for the Degree of*

Master of Technology

by

AJAY KUMAR



**DEPARTMENT OF MECHANICAL ENGINEERING
INDIAN INSTITUTE OF TECHNOLOGY , KANPUR**

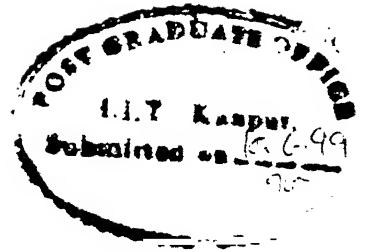
June, 1999

20 SEP 1992
CENTRAL LIBRARY
I. I. T., KANPUR
A 129316

TH
mf129316
K93p



2129316



CERTIFICATE

It is certified that the work contained in the thesis entitled, "A particle dynamics model for the evaluation of the performance of a Pelton Wheel bucket" by Ajay Kumar, has been carried out under ^{our} ~~my~~ supervision and this work has not been submitted elsewhere for a degree.

Dr. A. K. Mallik
Professor
Department of Mechanical Engg.
I. I. T. Kanpur

Dr. V. Eswaran
Associate Professor
Department of Mechanical Engg.
I. I. T. Kanpur

dedicated to
my parents

Acknowledgements

I would like to express my deep sence of gratitude and appreciation to my thesis supervisor Dr.V. Eswaran and Dr. A. Mallik for the skillful guidance, constant supervision, timely suggestions in carrying out the present work.

I extend my profound thanks to all my friends, who made my stay memorable one. I am very grateful to my colleagues Iftikhar Alam, Ritesh Nath and N.K.Prasad, summer trainee Monica and my senior P.N. JHA for the help I received from them.

It is difficult to find words to express my gratitude to Neha for her support in the last phase of this work. This work could not been completed without the blessings of my parents. Even to think of thanking them is to trivialise all that they have done for me. My profoundest debts to them therefore, remain silent and unacknowledged.

Ajay Kumar
IIT Kanpur
Junc, 1999

Contents

List of Figures	iii
List of Tables	iv
1 Introduction	1
2 Theoretical Formulation	6
2.1 Introduction	6
2.2 Kinematics and dynamics of a single particle for two-dimensional vane	6
2.2.1 Multi-particle system	12
2.2.2 Determination of initial position of a particle	13
2.2.3 Particle torque at the time of impact and after the impact .	14
2.3 kinematics and dynamics of a single particle for 3-dimensional bucket	15
2.3.1 Initial positions for multi-particle system and modelling of water jet shape	22
2.3.2 Torque applied at the time of impact and during subse- quent motion	24
3 Algorithm and test cases	25
3.1 Introduction	25
3.2 Runge-kutta (R-K) methods	26

3.3	Test case for RK4 solver	29
3.4	Test case2	30
3.5	Test case 3	33
3.6	Interpolation scheme for the surface of the bucket	36
3.7	Calculation of initial position for the series of particles	38
3.8	Discussion on a complete test case	39
3.9	Conclusion and future work	42
Bibliography		42

List of Figures

1.1	Schemetic diagram of Pelton wheel turbine	1
1.2	Schemetic diagram of pelton wheel bucket	2
2.1	Schematic diagram for 2D case at the time of impact	7
2.2	Schematic diagram for 2D case after impact	8
2.3	Multi-particle system	12
2.4	Initial and final position	13
2.5	Schematic diagram for 3D case	16
2.6	Water jet	22
3.1	Schematic diagram for 2D simple case	28
3.2	Schematic diagram for test case 2	30
3.3	Position of the particle	32
3.4	Angular veloctiy of particle	32
3.5	Accleration of particle	33
3.6	Schematic diagram for test case 3	34
3.7	Particles' time history	41
3.8	Particle's torque history	42
3.9	Particle's torque history on the bucket	42

List of Tables

3.1	For stationary vane	35
3.2	For moving vane	35

Abstract

The aim of the present work is to develop a computer program to compute the torque and power generated by a Pelton Wheel with a given bucket surface configuration. The water jet striking the Pelton Wheel buckets is modelled as a series of particles. The force and the torque exerted by every particle, both on impact and subsequently during the motion on vane, are computed, using Newtonian mechanics, at every instant of time and integrated over entire time span until they lose contact from the bucket. The time history of all particles are then used to obtain the total torque obtained by water jet, as a function of time. The bucket shape is taken to be arbitrarily specified in local spherical coordinates $r = f(\theta, \phi)$ for which data are supplied as rectangular grid ($M \times N$) in θ and ϕ having the value of r at every grid point. The aim is to help in the optimum design of Pelton Wheel buckets.

Chapter 1

Introduction

The purpose of a hydraulic turbine is to convert kinetic and potential energy of water into mechanical work. On the basis of the difference between the lower and higher water levels, known as head, three principal types of turbines - impulse turbine, the radial or mixed-flow reaction turbine, and the axial flow, or propeller, reaction turbine can be used.

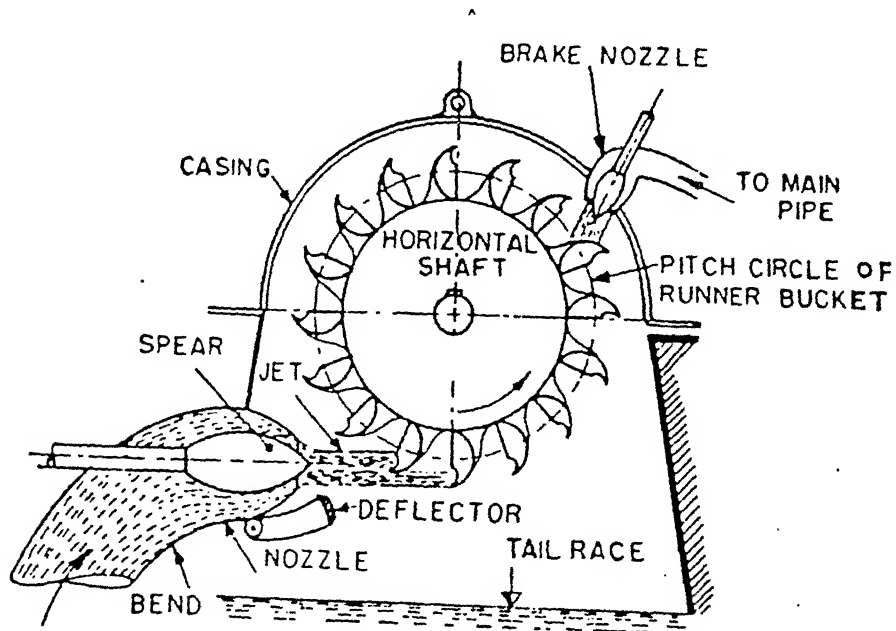


Figure 1.1: Schematic diagram of Pelton wheel turbine

Among the impulse water turbines, the Pelton turbine as shown in figure 1.1 is the only type being mostly used these days. It is also called the free jet turbine and operates under a high head and, therefore, requires a comparatively less flow rate of water. The head of the supply water is converted into one or more high-velocity free jets which are directed against buckets mounted on the rim of a wheel. The impact of water on the surface of the bucket produces a force which causes the wheel to rotate, thus supplying the mechanical power to the shaft.

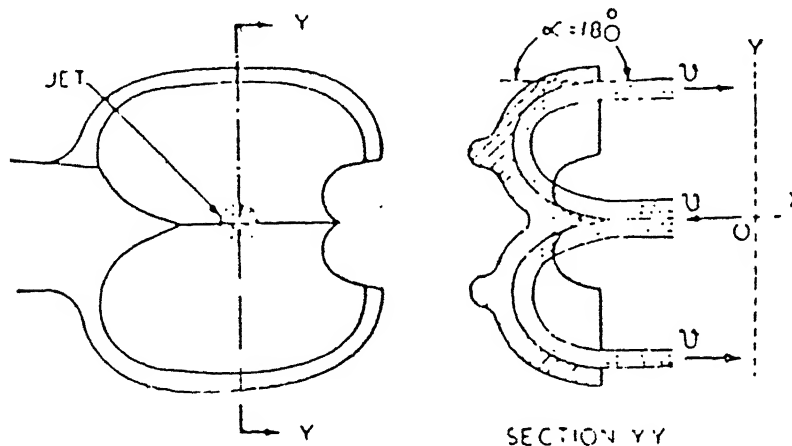


Figure 1.2: schematic diagram of pelton wheel bucket

In general, each bucket consists of two hemispherical cups separated by a sharp edge at the centre (see figure 1.2). The water jet impinges at the centre of the bucket and is divided by the sharp edge, without shock, into two parts moving sideways in opposite directions. The water after impinging on the buckets is deflected through an angle of about 165° instead of 180° as shown, so that it may

not strike the back of the other bucket and retard the motion of the wheel. The change in the momentum due to this change of directions transmits an 'impulse' torque on the bucket which translates to work output.

The efficiency of the wheel is given as

$$\eta = \frac{\text{work done on the bucket}}{\text{energy supplied to the bucket}}$$

The major problem is to find the power developed by a particular machine. The shape of the bucket plays a very important role in creating the torque. If the bucket surface is not proper, the water jet is not deflected smoothly with the result that there is needless dissipation of energy due to turbulence, and other irregularities in the bucket. More important, if the bucket is improperly shaped, the water flow does not undergo a sufficient deflection and hence generates less torque. So the optimum surface which gives maximum efficiency is required.

The efficiency of the Pelton wheel is generally very high (>90%). Therefore if improvement has to be made, we need to have analytical methods that can detect the effects of subtle changes in the bucket shape. In most text books, two dimensional analysis is presented using the velocity triangle for the calculation of work done on the bucket. This simple analysis using the velocity triangle is not adequate since it does not have any consideration of surface geometry except the deflected angle. Through experiments we can also analyse the effect of the bucket surface on the power developed by the wheel. But changing bucket parameters and doing experiment requires a lot of time as well as resources.

It would therefore, be of great help to the designer if a computational method can be found to theoretically evaluate the efficiency of a proposed bucket shape. The speed and relatively low cost of computational solutions will allow the designer to evaluate many possible bucket shapes before actually constructing prototypes for experimental testing. This problem, though an important one, has no published work. The commercial importance of the problem has ensured that any research on this problem is kept secret.

The general problem can be stated deceptively simply: Given a particular bucket shape, can its performance in terms of efficiency, torque, force and power generation can be predicted? The problem is a very difficult one. Any attempt to obtain answers through the traditional routes of fluid mechanics seems to be currently impossible- for the jet/bucket interaction involves a highly unsteady, even turbulent, flow in a complex geometry involving free surfaces. To attempt to solve for flow using Euler or Navier Stokes equations seems to be completely outside the scope of present-day computational fluid dynamics.

In this thesis a method, far simpler and probably more likely to succeed, is attempted. The jet is treated as a steady stream of perfectly plastic (i.e, deformable) "particles" which strike the bucket and slide on its surface imparting momentum and energy to the bucket. The motion of each such "particle" is taken to be independent of others and is computed using the Newtonian laws governing particle motion. These are coupled ordinary differential equations (much more numerically tractable than the partial differential equations of fluid flow) which can be solved by the Runge- Kutta method. However, considerable difficulty is introduced into the problem due to the generally complex bucket geometry involved. Once the time history of each particle is known from the solution of the dynamical equations, the effects of all particles can be integrated to obtain the total picture regarding the efficiency, torque etc., generated by the bucket.

In the present work, we have developed a computer program to analyse the performance of the buckets of general shapes of 2 and 3 dimensions. The torque imparted to the bucket is computed at every instant of time and integrated over entire time span.

The geometry of the bucket is usually very complex and is very important in the calculation of torque. In the present work, the surface of the bucket is represented in spherical coordinates (r, θ, ϕ) having uniform grid in θ and ϕ , with the value of r is specified at every grid point. Bicubic splines are used to find the interpolated value at any intermediate point. We can change the parameters of the bucket and see the effects on the torque developed. This analysis will help

selecting the optimum shape of the bucket. This work was partly supported by a project sponsored by BHEL, BHOPAL.

Chapter 2

Theoretical Formulation

2.1 Introduction

The water jet striking the Pelton Wheel buckets is modelled as a series of water particles. In this chapter, the kinematics and dynamics of the fluid particle for two dimensional (2D) and three dimensional (3D) situations are formulated. First we consider a 2D model for calculating the force and torque imparted on the rotating vane by a single particle. A general shape of the vane whose equation is given in polar coordinates is considered. Later, this 2D model is extended for a series of continuous particles and the concept of mass flow rate is introduced. Finally the general equations for 3D situations with any general shape of the bucket are obtained.

2.2 Kinematics and dynamics of a single particle for two-dimensional vane

Let us consider a two-dimensional vane rotating with a constant angular velocity $\omega \hat{k}$ about the point o as shown in figure 2.1 . A moving coordinate system having its origin at o' with $oo'=R$ attached to the vane. The equation of the vane profile

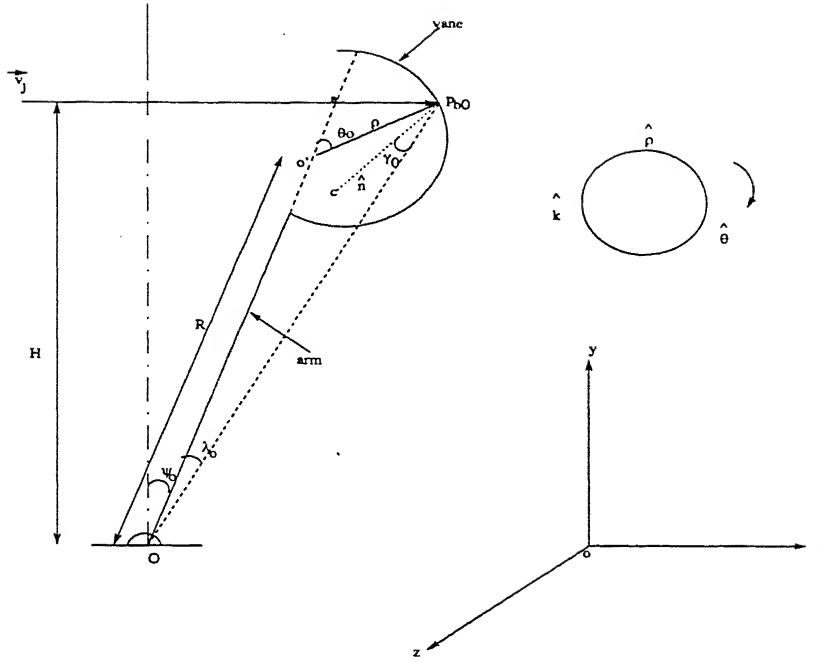


Figure 2.1: Schematic diagram for 2D case at the time of impact

in this moving coordinate system is described in polar form $\rho = \rho(\theta)$. Initially, at $t = t_{p0}$, let a particle (of water) strike the vane at the point p_{b0} with $\theta = \theta_0$. At this instant, the incoming absolute velocity of the particle is given by \vec{v}_j . The trajectory of this particle before striking the vane is horizontal and at a distance H from the axis of rotation (O) of the vane. The inclination of the arm from the vertical is ψ_0 (figure 2.1) which is known. It is easy to calculate θ_0 from geometry as follows from figure (2.1), and $\triangle O'ap_{b0}$

$$\frac{\cos \psi_0}{\rho(\theta_0)} = \frac{\cos(\psi_0 + \theta_0)}{\frac{H}{\cos \psi_0} - R}. \quad (2.1)$$

Equation (2.1) is solved numerically to obtain θ_0 from known values of H , R , ψ_0 and the given functional form of $\rho(\theta)$.

For all subsequent instants, we assume that the particle follows the vane profile until it loses contact, when the force exerted by the particle falls off to zero or

becomes negative. To obtain the location of the particle on the vane at subsequent time instants, i.e. $\theta(t)$ with the known values of θ_0 , we need to solve particle's dynamical equations as detailed below.

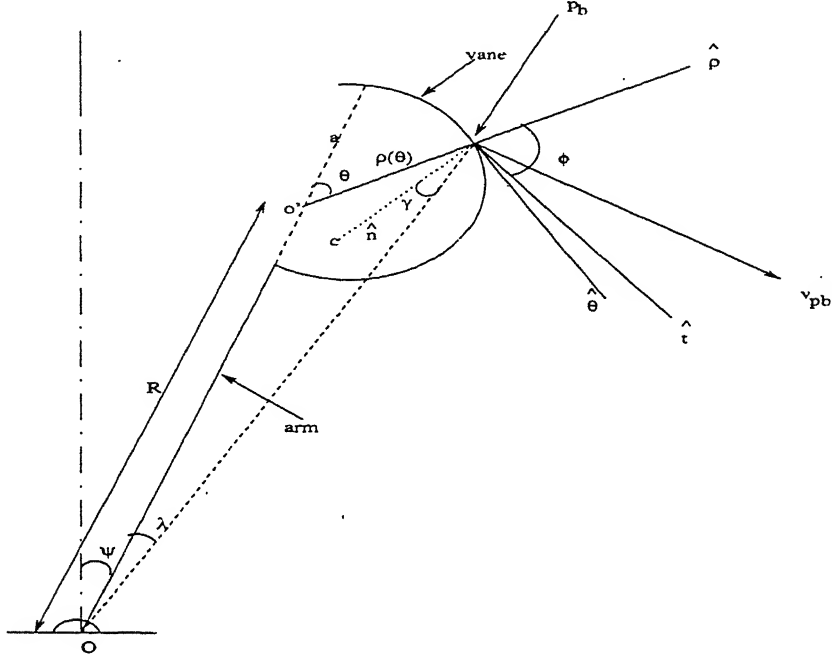


Figure 2.2: Schematic diagram for 2D case after impact

Referring to figure (2.2), let the point p_b on the vane indicates the location of the particle at any instant t . The point c' denotes the centre of curvature of the vane profile at the point p_b . The absolute acceleration of the particle at this instant is given by

$$\vec{a}_{abs} = \vec{a}_0 + \vec{\omega} \times (\vec{\omega} \times \vec{\rho}) + 2\vec{\omega} \times (\dot{\rho}\hat{\rho} + \rho\dot{\theta}\hat{\theta}) + (\ddot{\rho} - \rho\dot{\theta}^2)\hat{\rho} + (\rho\ddot{\theta} + 2\dot{\rho}\dot{\theta})\hat{\theta} \quad (2.2)$$

where, the acceleration of the point o is

$$\vec{a}_0 = \omega^2 R \cos(\pi - \theta)\hat{\rho} + \omega^2 R \cos(\frac{\pi}{2} - \theta)\hat{\theta} \quad (2.3)$$

Thus,

$$\begin{aligned}\vec{a}_{abs} &= (-\omega^2 R \cos \theta - \omega^2 \rho - 2\omega \rho \dot{\theta} + \ddot{\rho} - \rho \dot{\theta}^2) \hat{\rho} + (\omega^2 R \sin \theta + 2\omega \dot{\rho} + \rho \ddot{\theta} + 2\dot{\theta} \dot{\rho}) \hat{\theta} \\ &= a_\rho \hat{\rho} + a_\theta \hat{\theta}\end{aligned}\quad (2.4)$$

The components of \vec{a}_{abs} along \hat{n} and \hat{t} directions (the normal and tangent to the vane) are

$$a_n = -a_\rho \sin \phi + a_\theta \cos \phi \quad (2.5)$$

and

$$a_t = a_\rho \cos \phi + a_\theta \sin \phi \quad (2.6)$$

where ϕ , the angle between $\hat{\rho}$ and \hat{t} is obtained from

$$\cos \phi = \frac{\rho'}{\sqrt{\rho^2 + \rho'^2}} \quad (2.7)$$

$$\dot{\rho} = \rho' \dot{\theta} \quad (2.8)$$

and

$$\ddot{\rho} = \rho' \ddot{\theta} + \rho'' \dot{\theta}^2 \quad (2.9)$$

where ρ' is the derivative of ρ w.r.t. θ , and $\dot{\theta}$ and $\ddot{\theta}$ are the first and second derivative of θ w.r.t. time (t).

With the assumption of frictionless vane, it follows that the tangential acceleration a_t given by equation (2.6) is zero. Using equations (2.7)-(2.9), $a_t = 0$ reduces to

$$\ddot{\theta}(-\omega^2 R \cos \theta + \rho' \cos \phi) - (\omega^2 R \cos \theta + \omega^2 \rho + 2\omega \rho \dot{\theta} - \rho'' \dot{\theta}^2 + \rho \dot{\theta}^2) \cos \phi +$$

$$(\omega^2 R \sin \theta + 2\omega \rho' \dot{\theta} + 2\rho \dot{\theta}^2) \sin \phi = 0 \quad (2.10)$$

Equation (2.10) is a second order differential equation in θ only as ϕ can be obtained from the vane profile [see equation (2.7)] The ODE can be solved by using the fourth order Runge Kutta method (RK4) which will be discussed in detail in the next chapter. Since equation (2.10) is of second order, we need two initial conditions θ_0 and $\dot{\theta}_0$ (i.e., the value of θ and $\dot{\theta}$ at $t = t_{p0}$).

The value of θ_0 is known from equation (2.1) as stated earlier. To obtain the value of $\dot{\theta}_0$, it is assumed that after striking the vane, the velocity of the particle along the direction normal to the vane (\hat{n}) is given by that of the point p_{b0} along the same direction, whereas the component of \vec{v}_j along the \hat{t} direction remains unchanged. This assumes that the impact is perfectly plastic but frictionless.

Thus at $t = t_{p0}0^+$ (i.e., immediately after the impact), the velocity of the particle (see figure 2.1)

$$\begin{aligned} \vec{v}_{abs}^{0+} &= \omega \rho p_b \cos(\phi_0 + \theta_0 - \lambda_0) \hat{n} + v_j \sin(\theta_0 + \phi_0 + \psi_0) \hat{t} \\ &= (\omega \rho p_b \cos(\phi_0 + \theta_0 - \lambda_0) (-\sin \phi_0) + v_j \sin(\theta_0 + \phi_0) \\ &\quad \cos \phi_0) \hat{\rho} + (\omega \rho p_b \cos(\theta_0 + \phi_0 - \lambda_0) \cos \phi_0 + \\ &\quad v_j \sin(\phi_0 + \theta_0 + \psi_0) \sin \phi_0) \hat{\theta} \end{aligned} \quad (2.11)$$

where λ_0 is obtained as explained below.

From $\Delta oo'p_{b0}$ in figure (2.1) using sine laws we get

$$\frac{R}{\sin(\theta_0 - \lambda_0)} = \frac{\rho_0}{\sin \lambda_0} = \frac{op_{b0}}{\sin \theta_0} \quad (2.12)$$

From equation (2.12), given θ_0 , ρ_0 , R , we can solve for λ_0 and the distance op_{b0} .

Further, the absolute velocity of the particle at any instant can be written as

$$\vec{v}_{abs} = \vec{v}_0 + \vec{\omega} \times \vec{\rho} + \dot{\rho}\hat{\rho} + \rho\dot{\theta}\hat{\theta}, \quad (2.13)$$

where the velocity of the point o' is

$$\vec{v}_0 = \omega R \cos\left(\frac{\pi}{2} - \theta\right)\hat{\rho} + \omega R \cos\theta\hat{\theta}. \quad (2.14)$$

Using equation (2.14) in equation (2.13) and substituting $t = t_{p0}0^+$, i.e., $\theta = \theta_0$, $\dot{\theta} = \dot{\theta}_0$, we can write

$$\vec{v}_{abs}^{0+} = (\omega R \sin\theta_0 + \dot{\rho}_0)\hat{\rho} + (\omega R \cos\theta_0 + \omega\rho_0 + \rho_0\dot{\theta}_0)\hat{\theta}. \quad (2.15)$$

Now, the θ -component of \vec{v}_{abs}^{0+} from equations (2.11) and (2.15) we get

$$\dot{\theta}_0 = \frac{(\omega\omega p_b \cos(\theta_0 + \phi_0 - \lambda_0) \cos\phi_0 + v_j \sin(\theta_0 + \phi_0 + \psi_0) \sin\phi_0 - \omega\rho_0 - \omega R \cos\theta_0)}{\rho_0}, \quad (2.16)$$

which along with θ_0 gives the initial conditions for equation (2.10).

Thus, after solving equation (2.10) numerically, we get θ , $\dot{\theta}$ and $\ddot{\theta}$ at any instant t . Using these values, we get \vec{a}_{abs} from equation (2.4). In fact, only the normal component of \vec{a}_{abs} is sought ($\vec{a}_{abs}^t=0$). The force exerted by the single particle is given by

$$F^n = -m_p a_{abs}^n \quad (2.17)$$

where, m_p is the mass a single particle ($= \dot{m}_p \Delta t$, where \dot{m}_p is the mass flow rate of the jet).

The initial force exerted by the particle during the first impact at p_{b0} is obtained as

$$F_i^n = -m_p (\vec{v}_{abs}^{0+} - \vec{v}_j)^n \quad (2.18)$$

After obtaining $\theta(t)$, we can track the particle in the fixed frame with the origin

at o by writing its coordinates as

$$y(t) = R \cos(\psi_0 + \omega t) + \rho \cos(\theta + \psi_0 + \omega t) \quad (2.19)$$

$$x(t) = R \sin(\psi_0 + \omega t) + \rho \sin(\theta + \psi_0 + \omega t) \quad (2.20)$$

2.2.1 Multi-particle system

We consider the water jet as a series of particles. That is, particles keep striking and travelling along the vane one by one until they lose the contact from vane. At a given instant of time, a number of particles will be present on the vane and each particle has its own independent history. The particle forces are computed

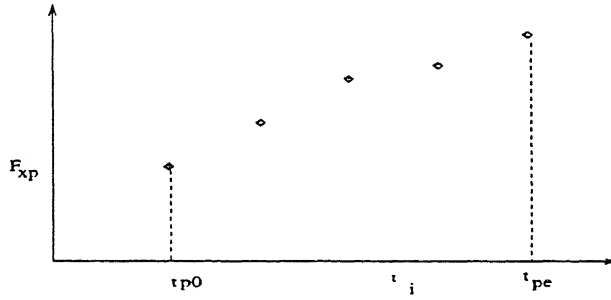


Figure 2.3: Multi-particle system

independently. At each time interval, for the given position of the vane, a particle is allowed to impact the vane. The entire time-history of that particle is then computed, along with the rotation of the vane, till the particle loses contact with the vane. The next particle is now calculated, starting with vane's position that is $\omega \Delta t$ after the previous position. This particle's time history is again calculated. Finally, after all the particles' histories are computed, the results are collated to find the force, say, at a particular time t .

Thus from the separate particle computations we obtain F_{xpi} , the force exerted by the particle at time t_i . After all the particle computations are done we know each F_{xpi} for $t_{p0} \leq t_i \leq t_{pe}$, where t_{p0} and t_{pe} are times at which the particle p

impacts, and leaves, the vane respectively. To find the force F_{xi} on the vane at time t_i , we have to find the sum

$$F_{xi} = \sum_p F_{pi} \text{ for all } p \text{ such that } t_{p0} \leq t_i \leq t_{pe}$$

A similar approach can be taken for the torque.

2.2.2 Determination of initial position of a paritcle

As shown in figure 2.4, the first particle strikes the vane when the arm makes an angle ψ_0 from the vertical and keep on striking one by one until the vane rotates away from the line of the jet. The vane rotates with angular velocity ω and angle ψ made by the arm with the vertical at any instant of time is $\psi_0 + \omega t$. The last particle strikes the vane when the arm has rotated to ψ_{max} given by

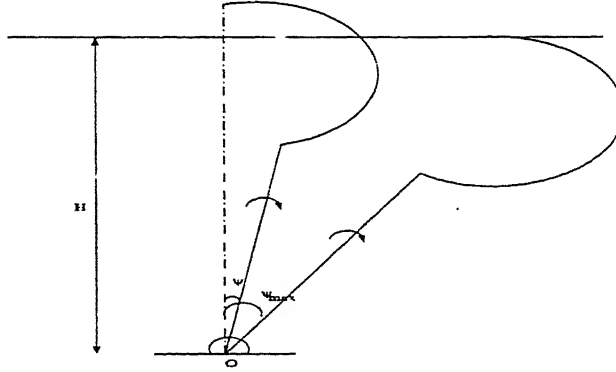


Figure 2.4: Initial and final position

$$\psi_{max} = \arccos\left(\frac{H}{\rho(\theta_0) - \rho(\theta_0)\cos(\theta_0)}\right)$$

For a given position of the vane, ψ , we want to find the θ where the particle will strike. From this, initial position of the particle path will be computed. From figure (2.2), in $\Delta o'ap_b$

$$\frac{\cos \psi}{\rho(\theta)} = \frac{\cos(\psi + \theta)}{\frac{H}{\cos \psi} - R}$$

or,

$$\rho(\theta) \cos(\psi + \theta) + R \cos \psi - H = 0 \quad (2.21)$$

With given $\rho(\theta)$, the value of θ satisfying equation (2.21) with $\psi = \psi_0 + \omega t$ gives the location at which the particle strikes.

2.2.3 Particle torque at the time of impact and after the impact

Momentum is imparted by the particle when it strikes the vane and also during the subsequent motion until the particle loses contact with the vane. Initial impact for a single particle having mass $m_p (= \dot{m}_p \Delta t)$, where \dot{m}_p is mass flow rate of jet, is given by

$$\begin{aligned} \vec{I}_{initial} &= -m_p(\vec{v}_{abs} - \vec{v}_j) \\ &= -m_p(\omega op_b \cos(\theta_0 + \phi_0 - \lambda) - v_j \sin(\theta_0 + \phi_0 - \frac{\pi}{2})) \end{aligned}$$

So torque imparted by the particle about the point o at the time of impact

$$\begin{aligned} M_{initial} &= I_{initial} op_b \sin \gamma_0 \\ &= -m_p(\omega op_b^2 \sin \gamma_0 (\cos(\theta_0 + \phi_0 - \lambda) - v_j \sin(\theta_0 + \phi_0 - \frac{\pi}{2}))) \end{aligned}$$

$$\text{with } \gamma_0 = \phi_0 + \theta_0 - \lambda_0 - \frac{\pi}{2}$$

The torque imparted by the particle about the point o at any instant during the motion of the particle on the vane is given by

$$M_{\Delta t} = -m_p a_n op_b \sin \gamma$$

To calculate the total torque imparted by the particle about the point o during its motion by the vane, we track the particle at every instant of time and sum up the torque to yield

$$\sum M_{\Delta t} = -m_p \sum a_n op_b \sin \gamma$$

We can obtain γ and op_b from the $\Delta oo'p_b$ in figure 2.2. Using sine laws we get

$$\frac{R}{\sin(\theta - \lambda)} = \frac{\rho(\theta)}{\sin \lambda} = \frac{op_b}{\sin \theta} \quad (2.22)$$

$$\text{and } \gamma = \phi + \theta - \lambda - \frac{\pi}{2}$$

So the net torque imparted by the particle is summation of the initial torque and on subsequent motion.

Thus, the net torque = $\sum M_{\Delta t} + M_{initial}$

2.3 kinematics and dynamics of a single particle for 3-dimensional bucket

Referring to figure (2.5) a, let us consider a bucket of general shape rotating with a constant angular velocity ω about the X-axis. There are two frames of reference considered, one fixed frame XYZ centered at o while another one moving frame xyz centered at o'. The frame xyz is attached to an extended point (o') of the arm whose distance from o is R. In figure 2.5 (b), the sign convention for spherical coordinates is shown. The surface equation of the bucket is assumed to be $\psi(r, \theta, \phi) = 0$ and when its gradient is given by

$$\nabla\psi = \frac{\partial\psi}{\partial r}\hat{r} + \frac{1}{r}\frac{\partial\psi}{\partial\theta}\hat{\theta} + \frac{1}{r\sin\theta}\frac{\partial\psi}{\partial\phi}\hat{\phi}$$

Initially at $t = 0$, the arm is assumed to make an angle χ_0 from the Z-axis, a particle travelling along the Y-axis strikes the bucket at point p_{b0} with velocity \vec{v}_j . The position vector of p_{b0} with respect to the moving frame is $r\hat{r}$. After striking the bucket at point p_{b0} , the particle is assumed to travel along the bucket. At that instant, absolute acceleration of the particle is along $-\nabla\psi$ (i.e. the bucket is assumed to be frictionless so the particle is subjected only to a normal force and experiences a normal acceleration) and given by

$$\vec{a}_{abs} = \vec{a}_0 + \vec{\omega} \times (\vec{\omega} \times \vec{r}) + 2\vec{\omega} \times (\dot{r}\hat{r} + r\dot{\theta}\hat{\theta} + r\sin\theta\dot{\phi}\hat{\phi}) + a_r\hat{r} + a_\theta\hat{\theta} + a_\phi\hat{\phi} \quad (2.23)$$

where \vec{a}_0 is the acceleration of point o'

$$\vec{a}_0 = -\omega^2 R \hat{k}$$

and a_r, a_θ, a_ϕ are the acceleration components of the point p_b in $\hat{r}, \hat{\theta}, \hat{\phi}$ directions, respectively. These components are given as

$$\begin{aligned} a_r &= \ddot{r} - r\dot{\theta}^2 - r\dot{\phi}^2 \sin^2 \theta \\ a_\theta &= r\ddot{\theta} + 2\dot{r}\dot{\theta} - r\dot{\phi}^2 \sin \theta \cos \theta \\ a_\phi &= r\ddot{\phi} \sin \theta + 2\dot{r}\dot{\phi} \sin \theta + 2r\dot{\theta}\dot{\phi} \cos \theta \end{aligned}$$

The relation between the cartesian coordinates and spherical coordinates for the moving frame are given as follows

$$\begin{aligned} \hat{r} &= \sin \theta \cos \phi \hat{i} + \sin \theta \sin \phi \hat{j} + \cos \theta \hat{k} \\ \hat{\theta} &= \cos \theta \cos \phi \hat{i} + \cos \theta \sin \phi \hat{j} - \sin \theta \hat{k} \\ \hat{\phi} &= -\sin \phi \hat{i} + \cos \phi \hat{j} \end{aligned}$$

The above relation can also be written as

$$\begin{Bmatrix} \hat{i} \\ \hat{j} \\ \hat{k} \end{Bmatrix} = \begin{bmatrix} \sin \theta \cos \phi & \cos \theta \cos \phi & -\sin \phi \\ \sin \theta \sin \phi & \cos \theta \sin \phi & \cos \phi \\ \cos \theta & -\sin \theta & 0 \end{bmatrix} \begin{Bmatrix} \hat{r} \\ \hat{\theta} \\ \hat{\phi} \end{Bmatrix} \quad (2.24)$$

So we finally write equation (2.23) as

$$\vec{a}_{abs} = A_r \hat{r} + A_\theta \hat{\theta} + A_\phi \hat{\phi} \quad (2.25)$$

where,

$$\begin{aligned} A_r &= -\omega^2 R \cos \theta - \omega^2 r (\cos^2 \theta \cos^2 \phi + \sin^2 \phi) - 2\omega r (\dot{\phi} \cos \theta \sin \theta \\ &\quad \cos \phi + \dot{\theta} \sin \phi) + (\ddot{r} - r\dot{\theta}^2 - r\dot{\phi}^2 \sin^2 \theta), \end{aligned} \quad (2.26)$$

$$\begin{aligned} A_\theta &= \omega^2 R \sin \theta + \omega^2 r \sin \theta \cos \theta \cos^2 \phi + \dot{\omega} r \sin \phi + 2\omega (r\dot{\phi} \sin^2 \theta \\ &\quad + \dot{r} \sin \phi) + (r\ddot{\theta} + 2\dot{r}\dot{\theta} - r\dot{\phi}^2 \sin \theta \cos \theta), \end{aligned} \quad (2.27)$$

and

$$A_\phi \doteq -\omega^2 r \sin \theta \cos \phi \sin \phi + \dot{\omega} r \cos \theta \cos \phi + 2\omega(\dot{r} \cos \theta \cos \phi - r\dot{\theta} \sin \theta \cos \phi) + (r\ddot{\phi} \sin \theta + 2\dot{r}\dot{\phi} \sin \theta + 2r\dot{\theta}\dot{\phi} \cos \theta). \quad (2.28)$$

The following two equations are obtained by assuming the bucket to be frictionless.

$$\frac{A_r}{\frac{\partial \psi}{\partial r}} = \frac{A_\theta}{\frac{1}{r} \frac{\partial \psi}{\partial \theta}} \quad (2.29)$$

and

$$\frac{A_r}{\frac{\partial \psi}{\partial r}} = \frac{A_\phi}{\frac{1}{r \sin \theta} \frac{\partial \psi}{\partial \phi}} \quad (2.30)$$

along with

$$\psi(r, \theta, \phi) = 0 \quad (2.31)$$

Substituting equation (2.31) in equations (2.29) and (2.30) we get

$$a_{11}\ddot{\theta} + a_{12}\ddot{\phi} + a_{13}\dot{\theta}^2 + a_{14}\dot{\phi}^2 + a_{15}\dot{\phi} + a_{16}\dot{\theta}\dot{\phi} + c = 0 \quad (2.32)$$

and

$$a_{21}\ddot{\theta} + a_{22}\ddot{\phi} + a_{23}\dot{\theta}^2 + a_{24}\dot{\phi}^2 + a_{25}\dot{\theta} + a_{26}\dot{\theta}\dot{\phi} + d = 0 \quad (2.33)$$

where,

$$\begin{aligned} a_{11} &= \left(-\frac{1}{r} \frac{(\frac{\partial \psi}{\partial \theta})^2}{\frac{\partial \psi}{\partial r}} - r \frac{\partial \psi}{\partial r} \right) \\ a_{12} &= -\frac{1}{r} \frac{\frac{\partial \psi}{\partial \theta} \frac{\partial \psi}{\partial \phi}}{\frac{\partial \psi}{\partial r}} \\ a_{13} &= \frac{2}{r} \frac{(\frac{\partial \psi}{\partial \theta})^2 \frac{\partial^2 \psi}{\partial r \partial \theta}}{\frac{\partial \psi}{\partial r}} - \frac{1}{r} \frac{\frac{\partial^2 \psi}{\partial r^2} (\frac{\partial \psi}{\partial \theta})^3}{(\frac{\partial \psi}{\partial r})^3} - \frac{1}{r} \frac{\frac{\partial^2 \psi}{\partial \theta^2} \frac{\partial \psi}{\partial \theta}}{\frac{\partial \psi}{\partial r}} + \frac{\partial \psi}{\partial \theta} \\ a_{14} &= 2 \frac{1}{r} \frac{\frac{\partial^2 \psi}{\partial r \partial \phi} \frac{\partial \psi}{\partial \theta} \frac{\partial \psi}{\partial \phi}}{(\frac{\partial \psi}{\partial r})^2} - \frac{1}{r} \frac{\frac{\partial^2 \psi}{\partial r^2} \frac{\partial \psi}{\partial \theta} (\frac{\partial \psi}{\partial \phi})^2}{(\frac{\partial \psi}{\partial r})^3} - \frac{1}{r} \frac{\frac{\partial^2 \psi}{\partial \phi^2} \frac{\partial \psi}{\partial \theta}}{\frac{\partial \psi}{\partial r}} - \sin^2 \theta \frac{\partial \psi}{\partial \theta} + r \sin \theta \end{aligned}$$

$$\begin{aligned}
& +r \sin \theta \cos \theta \frac{\partial \psi}{\partial r} \\
a_{15} &= -2\omega \cos \theta \sin \theta \cos \phi \frac{\partial \psi}{\partial \theta} - 2\omega r \sin^2 \theta \cos \phi \frac{\partial \psi}{\partial r} + 2\omega \sin \phi \frac{\partial \psi}{\partial \phi} \\
a_{16} &= \frac{2}{r} \frac{\frac{\partial^2 \psi}{\partial r \partial \theta} \frac{\partial \psi}{\partial \theta} \frac{\partial \psi}{\partial \phi}}{(\frac{\partial \psi}{\partial r})^2} + \frac{2}{r} \frac{\frac{\partial^2 \psi}{\partial r \partial \phi} (\frac{\partial \psi}{\partial \theta})^2}{(\frac{\partial \psi}{\partial r})^2} - \frac{2}{r} \frac{\frac{\partial^2 \psi}{\partial \theta \partial \phi} \frac{\partial \psi}{\partial \theta}}{\frac{\partial \psi}{\partial r}} - \frac{2}{r} \frac{\frac{\partial^2 \psi}{\partial r^2} (\frac{\partial \psi}{\partial \theta})^2 \frac{\partial \psi}{\partial \phi}}{(\frac{\partial \psi}{\partial r})^3} \\
& + 2 \frac{\partial \psi}{\partial \phi} \\
c &= -\frac{1}{r} \frac{\partial \psi}{\partial \theta} (\omega^2 R \cos \theta + \omega^2 r (\cos^2 \theta \cos^2 \phi + \sin^2 \phi)) - \frac{\partial \psi}{\partial r} (\omega^2 R \sin \theta \\
& + \omega^2 r \sin \theta \cos \theta \cos^2 \phi + \omega r \sin \phi) \\
a_{21} &= -\frac{1}{r \sin \theta} \frac{\frac{\partial \psi}{\partial \theta} \frac{\partial \psi}{\partial \phi}}{\frac{\partial \psi}{\partial r}} \\
a_{22} &= -\frac{1}{r \sin \theta} \frac{(\frac{\partial \psi}{\partial \phi})^2}{\frac{\partial \psi}{\partial r}} - r \sin \theta \frac{\partial \psi}{\partial r} \\
a_{23} &= \frac{2}{r \sin \theta} \frac{\frac{\partial^2 \psi}{\partial r \partial \theta} \frac{\partial \psi}{\partial \theta} \frac{\partial \psi}{\partial \phi}}{(\frac{\partial \psi}{\partial r})^2} - \frac{1}{r \sin \theta} \frac{\frac{\partial^2 \psi}{\partial r^2} (\frac{\partial \psi}{\partial \theta})^2 \frac{\partial \psi}{\partial \phi}}{(\frac{\partial \psi}{\partial r})^3} - \frac{1}{r \sin \theta} \frac{\frac{\partial^2 \psi}{\partial \theta^2} \frac{\partial \psi}{\partial \phi}}{\frac{\partial \psi}{\partial r}} - \frac{1}{\sin \theta} \frac{\partial \psi}{\partial \phi} \\
a_{24} &= \frac{2}{r \sin \theta} \frac{\frac{\partial^2 \psi}{\partial r \partial \phi} (\frac{\partial \psi}{\partial \theta})^2}{(\frac{\partial \psi}{\partial r})^2} - \frac{1}{r \sin \theta} \frac{\frac{\partial^2 \psi}{\partial r^2} (\frac{\partial \psi}{\partial \theta})^3}{(\frac{\partial \psi}{\partial r})^3} - \frac{1}{r \sin \theta} \frac{\frac{\partial^2 \psi}{\partial \theta^2} \frac{\partial \psi}{\partial \phi}}{\frac{\partial \psi}{\partial r}} + \sin \theta \frac{\partial \psi}{\partial \phi} \\
a_{25} &= -\frac{2\omega \sin \phi}{\sin \theta} \frac{\partial \psi}{\partial \phi} + 2\omega \cos \theta \cos \phi \frac{\partial \psi}{\partial \theta} + 2\omega r \sin \theta \cos \phi \frac{\partial \psi}{\partial r} \\
a_{26} &= \frac{2}{r \sin \theta} \frac{\frac{\partial^2 \psi}{\partial r \partial \theta} (\frac{\partial \psi}{\partial \phi})^2}{(\frac{\partial \psi}{\partial r})^2} + \frac{2}{r \sin \theta} \frac{\frac{\partial^2 \psi}{\partial r \partial \phi} \frac{\partial \psi}{\partial \theta} \frac{\partial \psi}{\partial \phi}}{(\frac{\partial \psi}{\partial r})^2} - \frac{2}{r \sin \theta} \frac{\frac{\partial^2 \psi}{\partial \theta \partial \phi} \frac{\partial \psi}{\partial \phi}}{\frac{\partial \psi}{\partial r}} - \frac{2}{r \sin \theta} \\
& \frac{\frac{\partial^2 \psi}{\partial r^2} \frac{\partial \psi}{\partial \theta} (\frac{\partial \psi}{\partial \phi})^2}{(\frac{\partial \psi}{\partial r})^3} - 2r \cos \theta \frac{\partial \psi}{\partial r} + 2 \sin \theta \frac{\partial \psi}{\partial \theta} \\
d &= \frac{1}{r \sin \theta} \frac{\partial \psi}{\partial \phi} (-\omega^2 R \cos \theta - \omega^2 r (\cos^2 \theta \cos^2 \phi + \sin^2 \phi)) - \frac{\partial \psi}{\partial r} (-\omega^2 r \\
& \sin \theta \cos \phi \sin \phi + \omega r \cos \theta \cos \phi)
\end{aligned}$$

Equation (2.32) and (2.33) are two coupled second order differential equations in θ and ϕ . So we need initial conditions θ_0 , ϕ_0 , $\dot{\theta}_0$ and $\dot{\phi}_0$ (i.e. the values of $\theta, \dot{\theta}, \phi$ and $\dot{\phi}$ at $t = t_{p0}$) as discussed in section 2.2. The value of θ_0 and ϕ_0 can be calculated from the following equations.

$$X_c = 0$$

$$Y_c = R \sin \chi_0 + z \sin \chi_0 + y \cos \chi_0$$

$$Z_c = H = R \cos \chi_0 + z \cos \chi_0 - y \sin \chi_0$$

where χ_0 is the angle made by the arm from the Z-axis when the particle

strikes. The methodology to solve the above equations and to get θ_0 and ϕ_0 will be discussed in detail later on.

To find the value of $\dot{\theta}$ and $\dot{\phi}$ at $t = 0$, we proceed as follows:

As discussed in the previous section, after the impact the component of jet velocity \vec{v}_j along $\nabla\vec{\psi}$ is same as the velocity of the point p_b in that direction but the velocity of the jet is unchanged in the direction normal to $\nabla\vec{\psi}$, i.e. tangential to the surface.

So after the initial impact at $t = 0^+$,

along $\nabla\vec{\psi}$, the component of \vec{v}_j = component of \vec{v}_{pb}

or,

$$\vec{v}_j - \frac{(\vec{v}_j \cdot \nabla\vec{\psi})\nabla\vec{\psi}}{|\nabla\vec{\psi}|^2} = \vec{\omega} \times R\hat{k} + \vec{\omega} \times r\hat{r} + \dot{r}\hat{r} + r\dot{\theta}\hat{\theta} + r\sin\theta\dot{\phi}\hat{\phi} \quad (2.34)$$

where

$$\vec{v}_j = v_j \cos\chi\hat{j} + v_j \sin\chi\hat{k}$$

The relations between the cartesian coordinates of the fixed frame and the moving frame are as follows;

$$\hat{I} = \hat{i}$$

$$\hat{J} = \cos\chi\hat{j} + \sin\chi\hat{k}$$

$$\hat{K} = -\sin\chi\hat{j} + \cos\chi\hat{k}$$

So from equation (2.34) we equate components on the left and right to find

$$\dot{\theta}_0 = \frac{-\omega R \cos\theta \sin\phi - \frac{\vec{v}_j \cdot \nabla\vec{\psi}}{|\nabla\vec{\psi}|^2} \frac{1}{r} \frac{\partial\psi}{\partial\theta} + v_j (\cos\chi \cos\theta \sin\phi - \sin\chi \sin\theta) - \omega r \sin\theta}{r} \quad (2.35)$$

and

$$\dot{\phi}_0 = \frac{-\omega R \cos\phi - \omega r \cos\theta \cos\phi + v_j \cos\chi \cos\phi + \frac{\vec{v}_j \cdot \nabla\vec{\psi}}{|\nabla\vec{\psi}|^2} \frac{1}{r \sin\theta} \frac{\partial\psi}{\partial\phi}}{r \sin\theta} \quad (2.36)$$

where,

$$\vec{v}_j \cdot \nabla \vec{\psi} = v_j \left((\cos \chi \sin \theta \sin \phi + \sin \chi \cos \theta) \frac{\partial \psi}{\partial r} + (\cos \chi \cos \theta \sin \phi - \sin \chi \sin \theta) \frac{1}{r} \frac{\partial \psi}{\partial \theta} + \cos \chi \cos \phi \frac{1}{r \sin \theta} \frac{\partial \psi}{\partial \phi} \right)$$

Using these initial conditions we solve equations (2.32) and (2.33) numerically we get $\theta, \dot{\theta}, \ddot{\theta}, \phi, \dot{\phi}$ and $\ddot{\phi}$ from the initial (impact) time t_{pi} to the time the particle leaves the bucket. The particle is considered to have left the vane whenever the computed a_n becomes positive. Using these values, we get \vec{a}_{abs} from the equation (2.25). The force exerted by the single particle is given by

$$F = -m_p a_{abs} \quad (2.37)$$

where, $m_p (= \dot{m}_p \Delta t)$ is the mass of the particle.

The initial impulse exerted by the particle during the first impact at p_{b0} is obtained as

$$I_n = m_p \left(\frac{\vec{v}_j \cdot \nabla \vec{\psi}}{|\nabla \vec{\psi}|} - \frac{\vec{v}_{pb} \cdot \nabla \vec{\psi}}{|\nabla \vec{\psi}|} \right) \quad (2.38)$$

and the average force is taken to be

$$F_n = \dot{m}_p \left(\frac{\vec{v}_j \cdot \nabla \vec{\psi}}{|\nabla \vec{\psi}|} - \frac{\vec{v}_{pb} \cdot \nabla \vec{\psi}}{|\nabla \vec{\psi}|} \right) \quad (2.39)$$

where

$$\vec{v}_{pb} = \vec{\omega} \times \vec{op}_b,$$

$$\vec{op}_b = R\hat{k} + r\hat{r}$$

2.3.1 Initial positions for 3D case and modelling of water jet shape

In section 2.2.1 the multiparticle system has been introduced and for 2D case. Since particles strike one by one and keep on sliding along the vane till they lose contact from it. The computation for each particle is done separately, from differ-

ent initial conditions. For a particle on centre line of the jet, the initial position where the particle strikes is:

$$X_c = 0$$

$$Y_c = R \sin \chi + z \sin \chi + y \cos \chi$$

$$Z_c = H = R \cos \chi + z \cos \chi - y \sin \chi$$

where, (X_c, Y_c, Z_c) is the point of impact with respect to fixed frame and $\chi = (\chi_0 + \omega t)$ is the angle shown in figure (2.5) which varies from χ_0 to χ_{max} , and (x_c, y_c, z_c) are the coordinates of the point of impact on the bucket surface in the moving coordinates system (figure 2.5).

It is however unlikely that particle will come only along the centre line, as the jet some finite radius l_0 . So we assume that the particle may come along a point randomly located on the circular cross-section of the jet. We do this by assigning a random position to the point by the prescription:

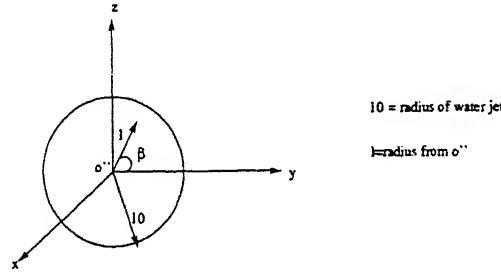


Figure 2.6: water jet

$$l = l_0 \sqrt{ran1}$$

$$\beta = 2\pi ran2$$

where $ran1$ and $ran2$ are two different uniformly distributed random numbers having values between $[0,1]$, the random point at any l and β are shown in figure (2.6). The square root in the prescription of l is to ensure that the points

are randomly distributed on the cross section. The initial position of the particles will be perturbed from the centre line by :

$$\Delta X = l \cos \beta$$

$$\Delta Z = l \sin \beta$$

where ΔX and ΔZ are the variation in X-direction and Z-direction, respectively, from the centre line. So now the equations for the initial positions are

$$X_p = \Delta X$$

$$Y_p = R \sin \chi + z \sin \chi + y \cos \chi$$

$$Z_p = H + \Delta Z = R \cos \chi + z \cos \chi - y \sin \chi$$

where (x, y, z) is the initial point in the moving frame which has to be determined for a given $\Delta X, \Delta Z, \chi, H$ and R . This requires the use of a root finding algorithm which will be explained later.

2.3.2 Particle torque computation in 3D case

In the same way as discussed in section 2.3.2 for the 2D case, we can calculate initial torque and on subsequent motion as follows:

Torque imparted by the particle about the X-axis at the time of impact

$$\vec{M}_{initial} = \vec{op}_b \times \vec{F}_i$$

Torque imparted by the particle about the X-axis during the motion on vane

$$\begin{aligned} \vec{M}_{\Delta t} &= m_p (\vec{op}_b \times \vec{a}_p) \\ &= m_p (-R \sin \theta A_\phi \hat{r} - (R \cos \theta + r) A_\phi \hat{\theta} + (A_\theta (R \cos \theta + r) + \\ &\quad A_r R \sin \theta) \hat{\phi}) \\ \sum M_{\Delta t} &= \sum m_p (\vec{op}_b \times \vec{a}_p) \\ &\quad m_p \sum (\vec{op}_b \times \vec{a}_p) \end{aligned}$$

So net torque = $\sum M_{\Delta t} + M_{initial}$

The total torque contribution of all particles can also be obtained in the same way as discussed in section 2.2.1.

Chapter 3

Algorithm and test cases

3.1 Introduction

This chapter presents the algorithm for particle tracking, force & moment calculations and for the integration of many particles information to obtain the overall torque. Towards the systematic development of the software, first of all the algorithm is developed for the 2D case and subsequently for the 3D case.

For each particle the path of the particle is computed by use of Newtonian dynamics. Subroutines were developed to compute the force exerted by the particle and its moment of momentum at time of impact and subsequently during the motion on vane. The torque exerted by all particles is summed up and related to the mass flow rate. The computer program is used to simulate problems with known analytical solutions and results were found to be perfectly matching for 2D circular and non-circular vanes.

The computer program was generalised to the 3D problem. The computer program was used to simulate the analytical results obtained previously and a perfect match was again found. The subroutines to compute torque etc., were extended to the 3D case so that the program can calculate, given the bucket shape, mass flow rate, the torque developed by the Pelton wheel.

3.2 Runge-kutta (R-K) methods

All the differential equations derived in chapter 2 are solved by using the fourth order Runge-Kutta 4 (RK-4) method. So RK-4 methods need a brief mention.

Runge-Kutta (R-K) methods are a one-step procedures which require only evaluation of first order derivatives, but which produce results equivalent in accuracy to the higher-order Taylor formulas. These methods are used to numerically solve ordinary differential equations (ODEs) of first order. Any ODE of higher order n is first reduced to a set of n first order ODE's and then solved.

A first-order initial value problem (IVP) is of the form

$$\frac{dy}{dx} = f(x, y); \quad y(x_0) = y_0; \quad x_0 \leq x \leq x_{max}. \quad (3.1)$$

Since, in general, the analytical solution cannot be obtained, the true solution $y(x)$ is approximated at $N + 1$ evenly spaced values of x , (x_0, x_1, \dots, x_N) , so that 'h' the step size is given by

$$h = \frac{x_{max} - x_0}{N} \quad (3.2)$$

$$x_{i+1} = x_i + h \quad (3.3)$$

where $i = 0, 1, \dots, N$

Beginning with the initial value of y_0 at the values of the solution y_1, y_2, \dots at the points x_1, x_2, \dots are computed sequentially according to the following rule:

$$y_{i+1} = y_i + \frac{h}{6}(K_1 + 2K_2 + 2K_3 + K_4) \quad (3.4)$$

where

$$K_1 = f(x_i, y_i)$$

$$K_2 = f\left(x_i + \frac{1}{2}h, y_i + \frac{1}{2}hK_1\right)$$

$$K_3 = f(x_i + \frac{1}{2}h, y_i + \frac{1}{2}hK_2)$$

$$K_4 = f(x_i + h, y_i + hK_3)$$

Consider the following system of n simultaneous first order ODE's:

$$\begin{aligned}\frac{dy_1}{dx} &= f_1(x, y_1, y_2, \dots, y_n) \\ \frac{dy_2}{dx} &= f_2(x, y_1, y_2, \dots, y_n) \\ &\vdots \\ \frac{dy_n}{dx} &= f_n(x, y_1, y_2, \dots, y_n)\end{aligned}\tag{3.5}$$

with initial conditions

$$\begin{aligned}y_1(x_0) &= y_{1,0} \\ y_2(x_0) &= y_{2,0} \\ &\vdots \\ y_n(x_0) &= y_{n,0}\end{aligned}\tag{3.6}$$

The solution of such a system is along the same lines as the solution of a single first order equation repeated n times. The R-K algorithm is applied to each of n equations in parallel at each step.

Consider a single higher order ODE

$$\frac{d^m y}{dx^m} = F(x, y, \frac{dy}{dx}, \frac{d^2 y}{dx^2}, \dots, \frac{d^{m-1} y}{dx^{m-1}})\tag{3.7}$$

with appropriate initial conditions for

$$y(x_0), \frac{dy(x_0)}{dx}, \dots, \frac{d^{m-1}y(x_0)}{dx^{m-1}}$$

The above ODE can be rewritten as a system of n simultaneous first order differential equations. Then the RK4 algorithm can be applied as above.

3.3 Two-dimensional simulations

Figure 3.1 shows the simplified schematic diagram of 2D case, having circular radius, at time of impact and after the impact.

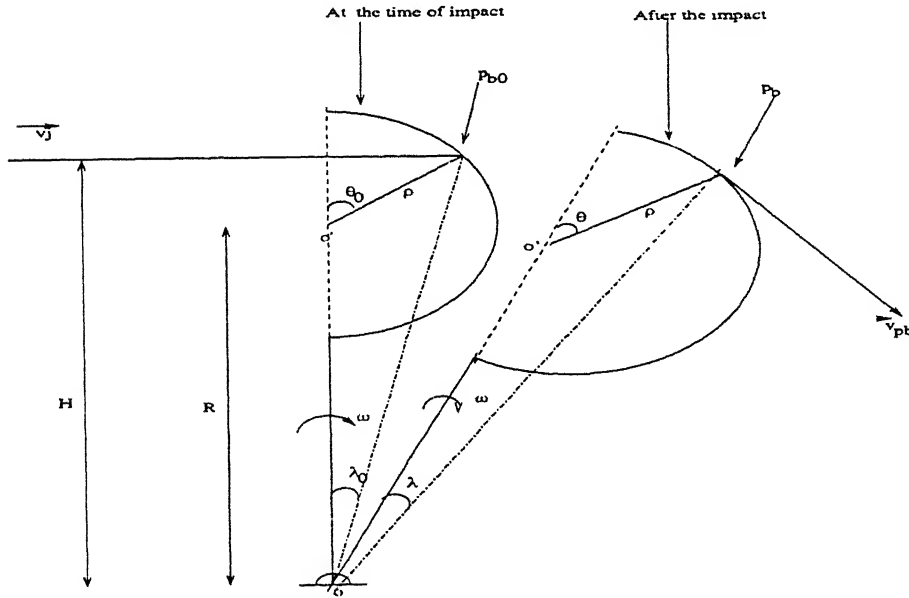


Figure 3.1: schematic diagram for 2D simple case

As discussed in section 2.2, we have a single second order ODE (after the

assumption that the vane is frictionless) which is given as

$$\ddot{\theta}(-\omega^2 R \cos \theta + \rho' \cos \phi) - (\omega^2 R \cos \theta + \omega^2 \rho + 2\omega \rho \dot{\theta} - \rho'' \dot{\theta}^2 + \rho \dot{\theta}^2) \cos \phi +$$

$$(\omega^2 R \sin \theta + 2\omega \rho' \dot{\theta} + 2\rho \dot{\theta}^2) \sin \phi = 0 \quad (3.8)$$

To track the particle at every instant of time, we need two initial conditions θ_0 and $\dot{\theta}_0$. The initial θ_0 is calculated as discussed in section 2.2. With the assumption, as discussed in section 2.2, that the velocity of the particle along the normal direction to the vane is given by that of the point p_{b0} , whereas the component along the tangential direction remains unchanged from the jet velocity, we get

$$\dot{\theta}_0 = \frac{(\omega \rho_b \cos(\theta_0 + \phi_0 - \lambda_0) \cos \phi_0 + v_j \sin(\theta_0 + \phi_0) \sin \phi_0 - \omega \rho_0 - \omega R \cos \theta_0)}{\rho_0} \quad (3.9)$$

So the computation is done in following way:

1. compute the initial conditions ($\theta_0, \dot{\theta}_0$)for the particle.
2. compute the initial impact force imparted by the particle.
3. compute the value of θ and $\dot{\theta}$ at next time step using previous step's θ and $\dot{\theta}$ and the RK4 solver.
4. compute the force and torque by the particle using the computed θ and $\dot{\theta}$.
5. step 3 and step 4 repeated until the force exerted by the particle falls off to zero.

3.4 Test case for RK4 solver

We assume the simplest case when there is no vane present to obstruct i.e. the particle is like a free particle as no force will be exerted on the particle, its absolute

acceleration will be zero and particle will move in a straight line.

In our numerical simulation we suppose a fictitious vane (see figure 3.1) having circular vane of radius $\rho = c$. So we solve equation (2.10) under following two initial conditions: $\theta = \theta_0$ and, from equation (2.16), $\dot{\theta}_0 = \frac{\cos \theta_0}{\rho} (v_j - \omega R) - \omega$, since $\psi_0 = 0$ and $\phi_0 = \frac{\pi}{2}$.

For different values of c , θ_0 , v_j , ω and R the equation (2.10) is solved having the time step $\Delta t = .01$. After solving the equation (2.10) for θ we track the particle at every instant of time using equations (2.19) and (2.20) and the path travelled by the the particle was found to be straight line. This validates the kinetics of the particle.

3.5 Test case2

This problem is selected to test the numerical solution against an analytical solution in a complex dynamic problem.

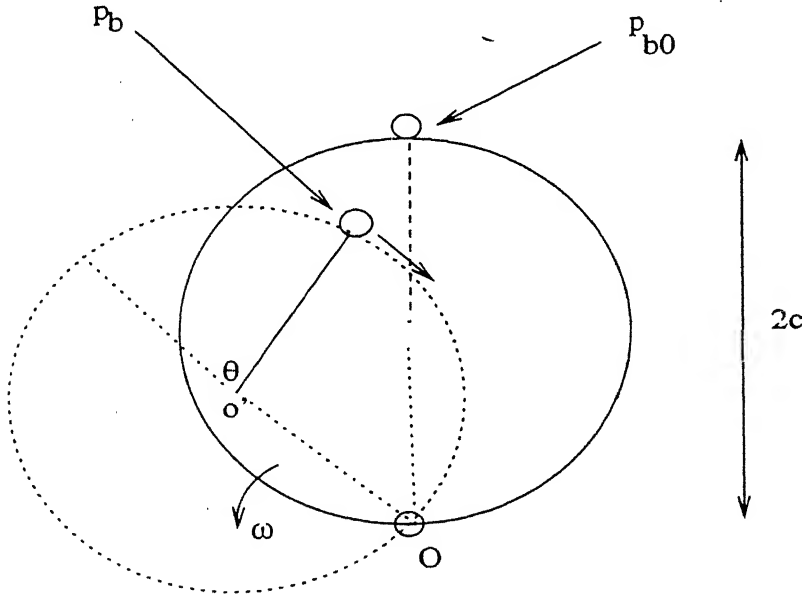


Figure 3.2: Schematic diagram for test case 2

A frictionless circular ring having diameter $2c$ and centre at o' is hinged at

point o. Initially a particle is at point p_{b0} at the diametrical distance from o as shown in figure (3.2) and the ring is at rest. At $t = 0$, the ring starts rotating counter clockwise at constant angular velocity ω_0 . At any instant of time the particle is at point p_b as shown in figure (3.2) whose position (θ), angular velocity ($\dot{\theta}$) and radial force (a_ρ) can be obtained analytically and are given as follows:

$$\theta = -4 \arctan(\exp(\omega_0 t) - \frac{\pi}{4})$$

$$\dot{\theta} = -\omega_0 \sqrt{2(1 + \cos \theta)}$$

$$a_\rho = \omega_0^2 c \left[2\sqrt{2(1 + \cos \theta)} - 3(1 + \cos \theta) \right]$$

The situation shown in figure 3.1 can be reduced to the situation as described in figure 3.2 by applying the following conditions: $v_j = 0$, $\omega = -\omega_0$, $\rho = c$ and $R - \rho = 0$. So equation (2.10) is solved using RK4 solver with following initial conditions:

$$\theta_0 = 0 \text{ and } \dot{\theta}_0 = 0$$

An angular velocity $\omega=2$, $c=5$ and time step $\Delta t = .01$ are used for computations. The results are shown in the following graphs.

The following graphs shows the perfect match between computed solution and analytical solution for θ , $\dot{\theta}$ and a_ρ . So this test validates the numerical solver for the equation (2.10) completely.

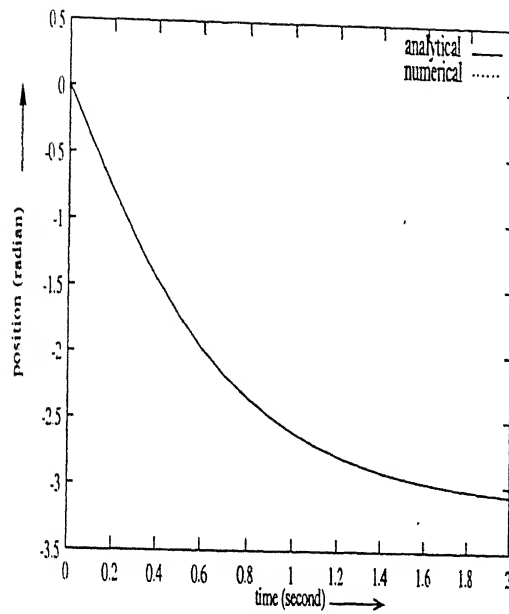


Figure 3.3: position of the particle

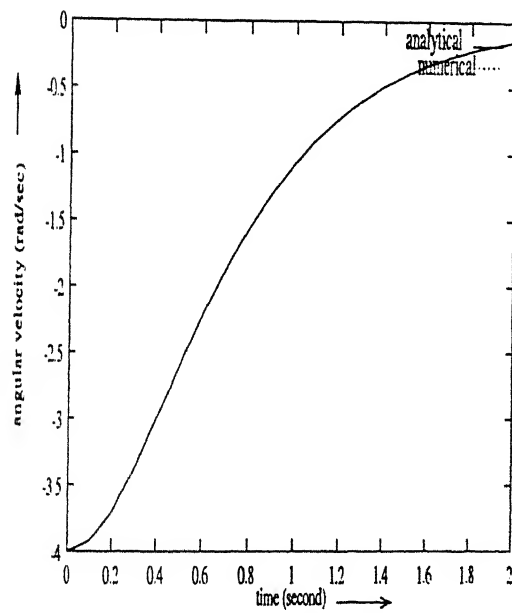


Figure 3.4: angular velocity of particle

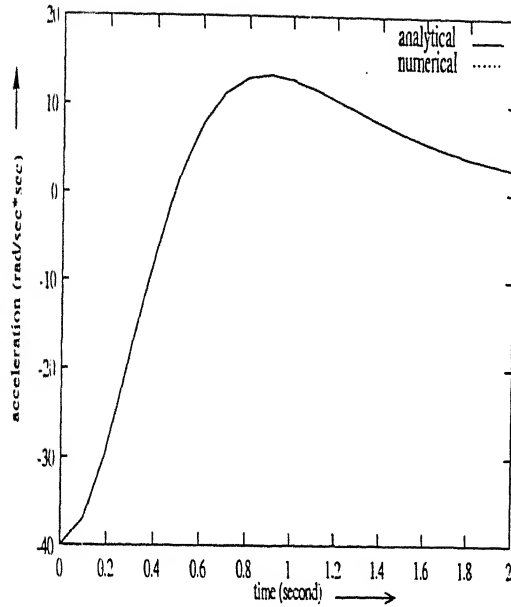


Figure 3.5: acceleration of particle

3.6 Test case 3

This problem is selected to check the computed force and torque applied by a jet against known analytical solutions for a 2D vane. An analytical solutions are not known for even the simplest cases of a rotating vane, we have considered two special cases for which such solutions are known: (a) a stationary vane and (b) a translating vane. These simple cases however allow us to check the numerical solution which is computed by essentially the same method (solving the ODE's etc) as are more realistic cases. The utility of this test is that in this case we check not only the particle dynamics but also the integration routines which collate all the particles information to give a composite picture of the force and torque on the entire vane.

Referring to figure (3.6), the vane has the shape of $\rho(\theta) = 1 + \cos \theta$. The water particle strikes the vane at point 'a' and after travelling along the vane it exits at 'b'.

case a: stationary vane

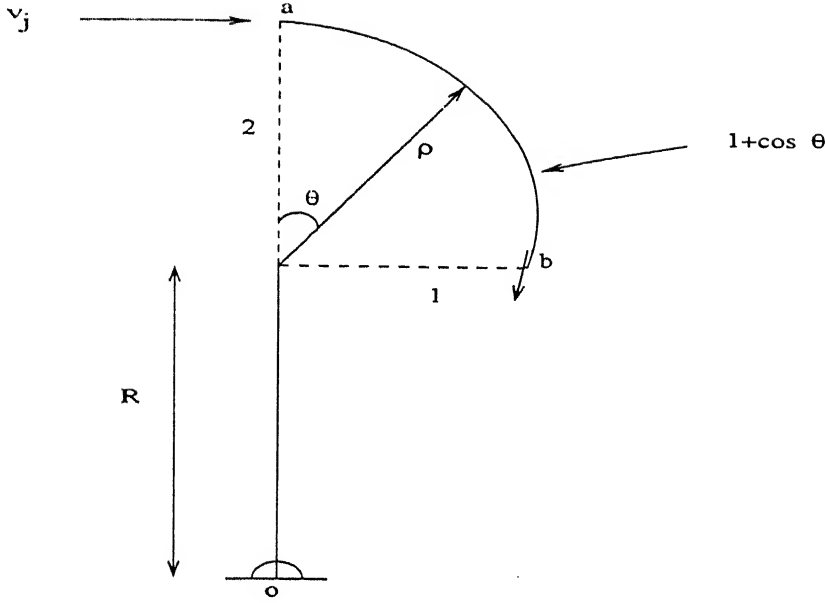


Figure 3.6: Schematic diagram for test case 3

For this case, the vane remains in the position shown in figure (3.6). The analytical solution for the force exerted along the X-direction (F_x) and the torque about the point 'o' are easily calculated as

$$F_x = \dot{m}v_j\left(1 + \frac{1}{\sqrt{2}}\right),$$

and

$$T = \dot{m}v_j \left[\left(\frac{R-1}{\sqrt{2}} \right) + (R+2) \right].$$

The program is simulated with following conditions: $\omega = 0$, $\dot{m} = 1$ and initial conditons $\theta_0 = 0$, $\rho = 2$ and $\dot{\theta} = \frac{v_j \sin^2 \phi_0 - 2\omega - \omega R}{2}$. Computations are done for different value of R and v_j and are given in the table (3.1).

Table (3.1) shows the perfect match between the analytical and computed solutions. The time step Δt is very important, for if particle comes with high velocity, it is going to take very little time to travel along the vane. So time step has to be

velocity(m/s)	R(m)	force(N) analytical	force(N) computed	torque(Nm) analytical	torque(Nm) computed	Δt time step
1	1	1.707200	1.70836	3	2.99881864	0.01
5	1	8.536000	8.53928	15	14.9941990	0.01
50	3	85.36000	85.42057	320.721344	320.791016	0.001
100	3	170.7200	170.8534	641.628784	641.442688	0.0001

Table 3.1: For stationary vane

smaller than the time step taken for relatively slower velocities.

case b: moving vane

When vane in Fig. (3.6) has a translational velocity v_0 . Then the force F_x is given by

$$F_x = \dot{m}_p (v_j - v_0) \left(1 + \frac{1}{\sqrt{2}}\right)$$

The computer program is simulated using following conditions:

$$R \rightarrow \infty, \omega \rightarrow 0 \text{ and initial conditions } \theta_0 = 0, \rho_0 = 2 \text{ and } \dot{\theta} = \frac{v_j \sin^2 \phi - 2\omega - v_0}{2}$$

and computation is done for different value of v_j , v_0 and \dot{m}_p and are shown in the table (3.2).The numerical solutions match very well with the analytical solution in this case also.

v_j (m/s)	v_0 (m/s)	\dot{m}_p (kg/sec)	force(N) analytical	force(N) computed	Δt
2	1	1	1.707200	1.7078361	0.01
10	5	5	42.68000	42.71034	0.01
50	20	5	256.0800	256.5815	0.001
100	30	5	597.5200	599.8303	0.0001

Table 3.2: For moving vane

The equations (2.32)and (2.33) derived for 3D situations were also simulated for the above test cases and a perfect match was found with the 2D numerical solution as well as with the analytical solution.

3.7 Interpolation scheme for the surface of the bucket

The shape of a Pelton wheel bucket is quite complex and cannot be represented by simple analytical function. To overcome this difficulty, the bucket surface is represented in the form $r = f(\theta, \phi)$ where data are supplied in the form of a rectangular grid ($M \times N$) in θ and ϕ and at each grid point the radial distance (r) is given. To calculate the value of r at any θ and ϕ we need some interpolation scheme.

We use the cubic spline interpolation scheme since it provides a superior approximation for functions that may have local abrupt changes. The objective in cubic splines is to derive a third order polynomial for each interval between grid points. In one-dimension the function would be

$$f_j(x) = a_j x^3 + b_j x^2 + c_j x + d_j \quad (3.10)$$

where $j (= 1, 2, 3 \dots, n)$

To develop cubic splines we have to solve $4n$ equations for the values of a_j, b_j, c_j, d_j for n intervals. These equations are obtained by imposing the conditions that the function yields the tabulated values at the grid points and also that the piece-wise functions have continuous first and second derivatives at the grid points.

The second derivatives of the above function can be represented using a first-order Lagrange interpolating polynomial as

$$f_j''(x) = f_j''(x_{j-1}) \frac{x - x_j}{x_{j-1} - x_j} + f_j''(x_j) \frac{x - x_{j-1}}{x_j - x_{j-1}} \quad (3.11)$$

where $f_j''(x)$ is the value of the second derivative at any point x within the j^{th} interval. Integrating the equation (3.11) and using function equality conditions i.e. that $f(x_{j-1})$ must equal the tabulated f_j and $f(x_j)$ must equal f_{j+1} , and invoking the conditions that the first derivatives at grid points must be equal i.e.

$f'_j(x_j) = f'_{j+1}(x_j)$, we get

$$\begin{aligned} & \frac{x_j - x_{j-1}}{6} f''(x_{j-1}) + \frac{x_{j+1} - x_{j-1}}{3} f''(x_j) + \frac{x_{j+1} - x_j}{6} f''(x_{j+1}) \\ = & \frac{f(x_{j+1}) - f(x_j)}{x_{j+1} - x_j} - \frac{f(x_j) - f(x_{j-1})}{x_j - x_{j-1}} \end{aligned} \quad (3.12)$$

These $n-2$ linear equations have n unknowns, all the $f''(x_j)$'s. So setting $f''(x_1)$ and $f''(x_n)$ to zero, which gives the so-called natural spline which has zero second derivatives its boundaries, the above equations can easily be solved by using tridiagonal algorithm (TDMA).

In two dimensional interpolation, we seek an estimate of $f(\theta, \phi)$ from 2-dimensional rectangular grid ($M \times N$) of tabulated values of each of each of the independent variables θ, ϕ . To interpolate one functional value, i.e., of r , we perform M one dimensional splines evaluation across the rows of the table, followed by one additional one-dimensional splines down the newly created column. This is called bi-cubic spline interpolation.

Our primitive equations (2.32) and (2.33) for 3D computation contains the terms $\frac{\partial \psi}{\partial r}, \frac{\partial \psi}{\partial \theta}, \frac{\partial \psi}{\partial \phi}, \frac{\partial^2 \psi}{\partial r^2}, \frac{\partial^2 \psi}{\partial \theta^2}, \frac{\partial^2 \psi}{\partial \phi^2}$ and $\frac{\partial^2 \psi}{\partial \theta \partial \phi}$. As discussed earlier we have reduced $\psi(r, \theta, \phi)$ to $r - f(\theta, \phi)$. So $\frac{\partial \psi}{\partial r} = 1, \frac{\partial^2 \psi}{\partial r^2} = 0, \frac{\partial^2 \psi}{\partial r \partial \theta} = 0, \frac{\partial \psi}{\partial \theta} = -\frac{\partial f}{\partial \theta}, \frac{\partial \psi}{\partial \phi} = -\frac{\partial f}{\partial \phi}, \frac{\partial^2 \psi}{\partial \theta^2} = -\frac{\partial^2 f}{\partial \theta^2}, \frac{\partial^2 \psi}{\partial \phi^2} = -\frac{\partial^2 f}{\partial \phi^2}$ and $\frac{\partial^2 \psi}{\partial \theta \partial \phi} = -\frac{\partial^2 f}{\partial \theta \partial \phi}$.

To obtain the first, second and cross derivative with respect to θ and ϕ , at any point we apply finite difference scheme as we know the value of $f(\theta, \phi)$ at any point on given domain by using bi-cubic spline interpolation. So we can write

$$\begin{aligned} \frac{\partial f(\theta_i, \phi_j)}{\partial \theta} &= \frac{f(\theta_i + \Delta\theta, \phi_j) - f(\theta_i - \Delta\theta, \phi_j)}{2\Delta\theta} \\ \text{and } \frac{\partial^2 f(\theta_i, \phi_j)}{\partial \theta^2} &= \frac{f(\theta_i + \Delta\theta, \phi_j) - 2f(\theta_i, \phi_j) + f(\theta_i - \Delta\theta, \phi_j)}{\Delta\theta^2} \text{ etc.} \end{aligned}$$

where $\Delta\theta$ is a very small value. We use bi-cubic splines to evaluate all the functional values $f(\theta, \phi), f(\theta + \Delta\theta, \phi)$ etc and finally get the first and second derivative with respect to θ . Similarly we can calculate first and second derivative with respect to ϕ and also the cross-derivative. The computed value of first derivative and second derivative of $f(\theta, \phi)$ with respect to θ and ϕ is found to

be very close to the analytical solution for any smooth function but cross derivative ($\frac{\partial^2 f}{\partial \theta \partial \psi}$) does not match well. This is a fundamental problem with the bicubic spline because this representation does not account for cross terms. Since in equation (2.32) and (2.33) cross derivative comes only once as summation term, it does not affect the final solution very much. However, it is recommended that the program should be improved by using rational B-splines to represent the bucket surface instead of bi-cubic splines.

3.8 Calculation of initial position for the series of particles

Before the calculation for a particle can start we need to know its initial conditions, i.e., its initial position and velocity, both radial and angular need to be known. For a vane of complex geometry the first difficulty that arises is to find where the particle strikes the vane. As the vane is constantly moving, it has a different position for each particle. To calculate the initial position of particles in the spherical coordinates of the moving frame, the following methodology is used:

Referring to figure 2.5 (a) and 2.5 (b) the position of the particle in the fixed frame of reference is given below as discussed in section 2.3.1.

$$X_p = \Delta X \quad (3.13)$$

$$Y_p = R \sin \chi + z \sin \chi + y \cos \chi \quad (3.14)$$

$$Z_p = H + \Delta Z = R \cos \chi + z \cos \chi - y \sin \chi \quad (3.15)$$

We know the value of ΔX , $H + \Delta Z$, χ and R for every particle as discussed in section 2.3.1. Equations (3.13), (3.14) and (3.15) can be cast as follows:

$$x = X_p \quad (3.16)$$

$$y = Y_p \cos \chi - Z_p \sin \chi \quad (3.17)$$

$$z = Y_p \sin \chi + Z_p \cos \chi - R \quad (3.18)$$

The equation of surface $\psi(r, \theta, \phi) = 0$ can be cast as $\psi(x, y, z) = 0$.

Using equations (3.16), (3.17) and (3.18) we can cast the equation $\psi(x, y, z) = 0$ as

$$\psi(X_p, Y_p, Z_p) = 0 \quad (3.19)$$

In equation (3.19) X_p and Z_p are known, hence Y_p is the root of the equation (3.19). It can be solved by using NEWTON-RAPHSON scheme. After getting Y_p we can get θ and ϕ by back substitution.

For 3D computation, we have represented $\psi(r, \theta, \phi)$ as $r - f(\theta, \phi)$ and data are supplied in the form of rectangular grid ($M \times N$) in θ and ϕ and at each grid point the radial distance (r) is given. To find the value of θ and ϕ at the time of impact for each particle we follow the following procedure.

First of all, we convert the rectangular grid in θ and ϕ into the rectangular grid in X_p and Z_p having the value of Y_p at each grid point using equations (3.13)-(3.15). For a given value of X_p and Z_p we interpolate the value of Y_p using bi-cubic spline. Now we can calculate the value of x, y, z in moving frame using equations (3.13), (3.14) and (3.15) and from known value of x, y, z we calculate the value of r, θ and ϕ .

3.9 Discussion on a complete test case

The following steps are taken for entire computation.

step 1 - grid generation in θ and ϕ from given x, y, z points.

step 2 - computation of a number (n) of particles striking the bucket after assuming the time step (Δt) and starting angle of rotation (ψ_0) for given angular velocity of bucket (ω).

step 3 - initial condition ($\theta_0, \phi_0, \dot{\theta}_0$ and $\dot{\phi}_0$) of the particle is computed.

step 4 - initial momentum is computed for the particle.

step 5 - use the RK4 solver to compute the value of $\theta, \phi, \dot{\theta}$ and $\dot{\phi}$ for next time step.

step 6 - force by the particle is computed and checked whether it is less than zero or not. If the force is zero that means it has left the bucket.

step 7 - repeat step 5 and step 6 for the particles present in the bucket at that time step.

step 8 - repeat step 3 to 7 till all particles strike the bucket.

step 9 - collate all particle information to obtain the overall force, torque, power, efficiency, etc.

We have taken a test case for a hemispherical bucket. The parameters are as follows:

velocity of jet striking the bucket $v_j = 10\text{m/s}$.

angular velocity of bucket $\omega = 3\text{ rad/sec}$

The height at which jet strikes $H = 1.7\text{m}$

Time step $\Delta t = 0.01\text{ sec}$.

mass flow rate $\dot{m}_p = 2\text{ kg/s}$

The bucket starts from $\psi_0 = -\frac{\pi}{6}$ to $\frac{\pi}{6}$

Number of particle striking the bucket $n = 34$

power developed by wheel $= 35.58\text{ w}$

Efficiency of the bucket obtained is $= 37.018\%$

We tracked the every particle at every instant of time and torque is computed using above algorithm. The figure (3.7) shows time history of all particles hitting the bucket. Particles strike the bucket at every time instant and after travelling along the bucket they lose the contact. So figure (3.7) shows that maximum number of particles present in bucket is no more than 25 at a time while number of particle

striking the bucket are 34.

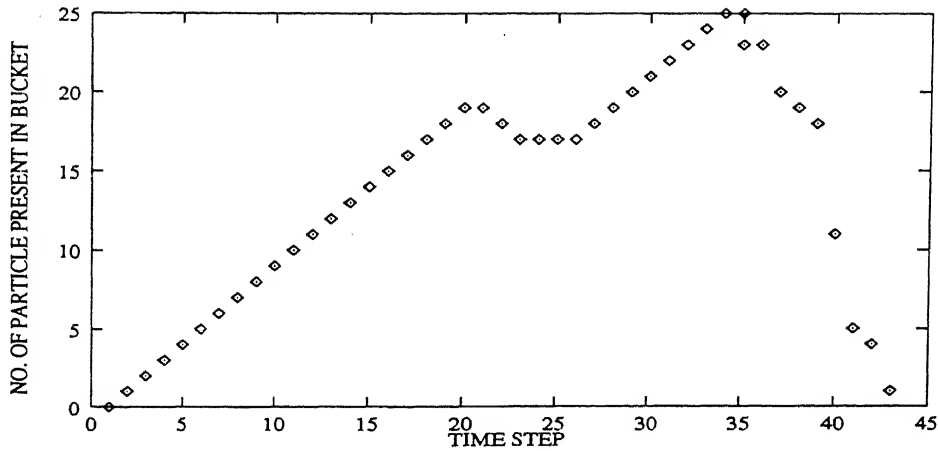


Figure 3.7: Particles' time history

Figure (3.8) shows the torque history of a particular particle over entire time span, starting from the initial impact till it loses the contact form the bucket. Although the efficiency of the hemispherical bucket is very low but this test case shows the general behaviour (as shown in figure 3.8) of the Pelton wheel that the maximum energy is transfered during the impact and slowly it falls off to zero. As discussed in chapter 1, the maximum energy can be transferred when the particle exactly bounces back in the opposite direction. But to avoid the interference from incoming flow, particle is deflected through some angle. Here the surface geometry comes in the picture.

Figure (3.9) shows the torque history of particle during its motion on vane. It clearly shows that a substantial amount of energy is transferred during the particle's motion on the vane. So depending upon the bucket shape, this energy can be enhanced. So a lot of improvement can be predicted on the basis of this analysis.

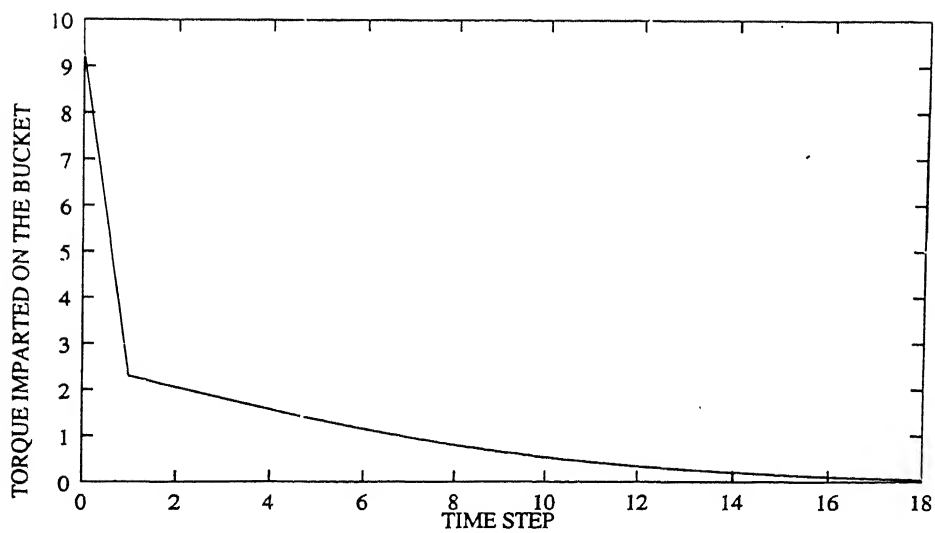


Figure 3.8: particle's torque history

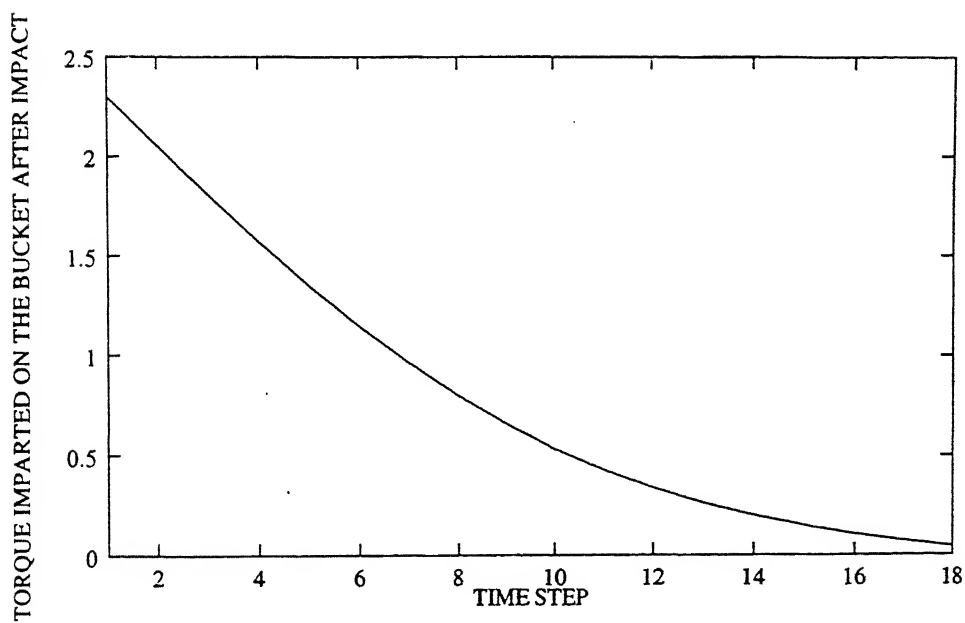


Figure 3.9: Particle's torque history on the bucket

3.10 Conclusion and future work

In this thesis, the torque is calculated for a single bucket having simple geometrical configuration. The scheme can be used to test the complex geometry. The scheme can also be easily extended for multi-bucket system.

In the future work, attention can be paid upon complexity of the geometry of the bucket like, the sharp edge in the centre of bucket and cut on the top of the bucket. The present work can be extended for non-friction surface. Attention can also be paid upon the water jet which is assumed to be running in straight line while in reality it has some curvature.

Bibliography

1. Ferdinand P.Beer and E.Russell Johnsson, Jr., Vector Mechanics for engineers, McGraw-Hill Book Company.
2. K.Murlidhar and T.Sundarajan, Numerical Fluid Flow and Heat transfer, Narosa Publishing House.
3. A.K.Jain, Fluid Mechanics, Khanna publishers, New Delhi.
4. Jagdish Lal, Hydraulic Machines, Metropolitan book co. pvt. Ltd., New Delhi